ELSEVIER

Polymer 41 (2000) 6573–6580

polymer

Molecular mobility of end allyl radicals of diene polymers tethered on a poly(tetrafluoroethylene) surface

K. Yamamoto[a], S. Suenaga[a], S. Shimada[a,*], M. Sakaguchi[b]

[a]*Nagoya Institute of Technology, Gokiso-cho, Showa ward, Nagoya 466-8555, Japan*
[b]*Ichimura Gakuen College, Uchikubo 61, Inuyama 484-8503, Japan*

Received 16 September 1999; received in revised form 8 November 1999; accepted 24 November 1999

Abstract

Poly(butadiene) (PBD), polyisoprene and poly(2-methyl pentadiene) (PMPD) tethered on a poly(tetrafluoroethylene) (PTFE) surface were produced by a mechanical fracture of PTFE powder with butadiene, isoprene and 2-methyl-1,3-pentadiene monomer at 77 K, respectively. The tethered polymer has an unpaired electron (allyl radical) at the chain end. The allyl radical was used as a label of molecular motions of the end. The e.s.r. spectral change was observed in the temperature range of 77–223 K and assigned to molecular motions which were a conformation exchange and a rotational motion of allyl radicals (around C–C bond). The rotational motion of PBD radicals was the most vigorous among the three polymers. In contrast the e.s.r. spectral change for PMPD radicals was little observed and the mobility was the least. Moreover, the motions of end allyl radicals were accelerated by the residual monomer.

Keywords: Diene polymer; Poly(tetrafluoroethylene) surface; Molecular motion

1. Introduction

Much attention has been paid recently to the molecular structures and the physical properties of single polymer chain. Atomic force microscopy [1–3] (AFM) and scanning tunneling microscopy [4] (STM) allowed the observation of directly absorbed structures of a single polymer chain on an inorganic surface. By means of AFM, the spatial density of the isolated single polymer on a surface was reported to be smaller than the bulk [5], and an entropic elasticity [6] was directly measured in an aqueous condition on a mica surface. We reported the molecular mobilities of the several isolated polymer chains were very high as indicated by e.s.r. The high mobility was associated with the density of the chains [7–11]. Thus, the properties of the isolated polymers are different from those of the bulk. It is important to investigate and understand the physical properties and the molecular structure of an isolated single polymer in order to develop an excellent material.

Radicals produced by a mechanical fracture of poly(tetrafluoroethylene) (PTFE) can initiate radical polymerization [12]; the radical concentration is low [13]. The polymer produced by the mechanical fracture is tethered on and located at the PTFE surface [14]. The tethered polymer is present in low concentrations, which is in the range of no contact with the neighboring tethered chains. The polymer chain mentioned here was regarded as an isolated polymer chain. We reported the molecular motion of various polymer chains tethered on a PTFE surface in an extremely low segmental density of the tethered polymer chain [7]. The tethered polymer chain has a higher mobility than the bulk polymer chain because of its lower segmental density. The mobility of the isolated polymer chain is non-cooperative and it was interpreted in terms of the conformer size concerned with the size of the repeat unit. As the intermolecular interactions of the chain are ignored in the isolated system, an intramolecular interaction can be studied. The above results are associated with the intramolecular interaction and will provide fundamental and important information on the polymer properties.

We reported the conformation exchange (site exchange) motion of end radicals of isolated polybutadiene (PBD) chains tethered on the PTFE surface and the effect of segmental density around the PBD chains on the motion below the melting point of 1,3-butadiene (BD) monomer. The rate of the motion was reduced by the solid monomer around the PBD chains [8].

The purpose of the present paper is to investigate the molecular mobility of end allyl radicals of diene polymers, PBD, polyisoprene (PIP) and poly(2-methyl pentadiene) (PMPD), which have no contact with each of the tethered

* Corresponding author. Tel.: +81-52-735-5263; fax: +81-52-735-5294.
E-mail address: shimada@mse.nitech.ac.jp (S. Shimada).

0032-3861/00/$ - see front matter
PII: S0032-3861(99)00879-4

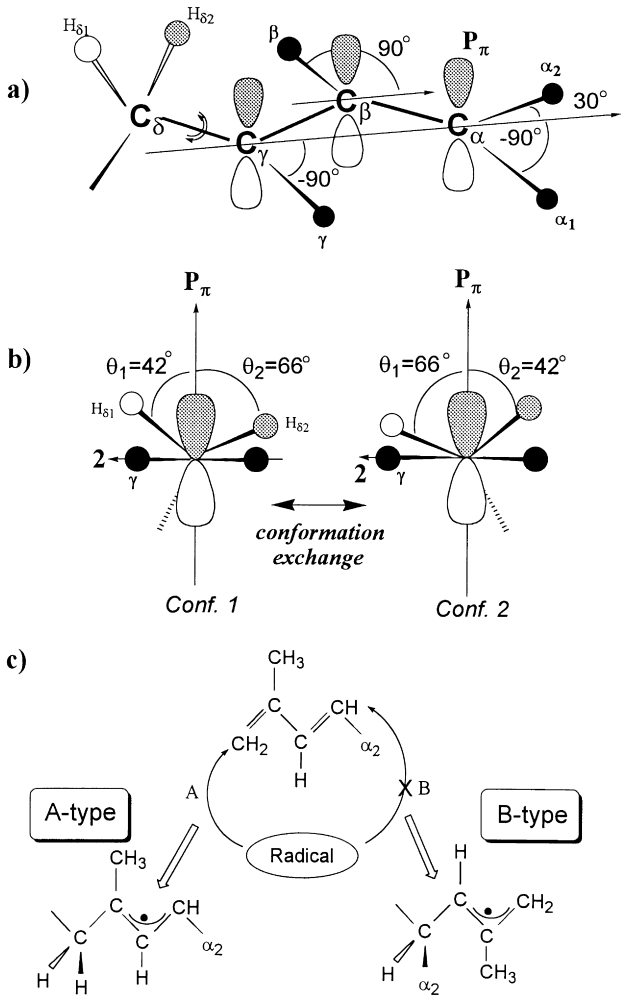

Fig. 1. (a) The coordinate system; (b) two conformations of end allyl radicals of diene polymers; and (c) two possible routes of the radical attack for asymmetric dienes.

chains. We report a relationship between the mobility of end allyl radicals and their structure and also discuss the influence of the amount of residual monomer on the mobility as the tethered polymers exist in an extremely low concentration on the PTFE surface.

2. Experimental

PTFE powder (Fluon G163, Asahi Glass Co., Ltd) was used without further purification. BD (Tokyo Chemical, Inc.), isoprene (IP) (Nacalai Tesque, Inc.) and 2-methyl-1,3-pentadiene (MPD) (Tokyo Chemical) were purified by a freeze–pump–thaw method.

The PBD, PIP and PMPD tethered chains on the PTFE surface were produced by a mechanical fracture of PTFE powder (1.50 g) with BD, IP and MPD, respectively, (approximately 5×10^{-5} to 10^{-3} mol) at 77 K in vacuum by a home-made glass ball mill [15]. The ball-milling of PTFE powder produces PTFE mechano radicals that are trapped on the PTFE surface and can initiate radical polymerization of diene monomers at 77 K when the monomer has contact with the mechano radicals by physical mixing during the milling. The radical polymerization of the diene monomer proceeds and the diene polymers tethered on the PTFE surface are produced. These polymers have an unpaired electron at the propagating ends which is used as a label of the molecular motions. After the polymerization, the e.s.r. sample tube connected to glass ball mill was placed in liquid nitrogen and the milled sample was dropped into the sample tube within 1 s by turning it upside down. The samples are named PTFE/M(*A*) in this paper, where M represents monomers (BD, IP and MPD) and *A* in the parenthesis represents the initial monomer amount (mol). In the case that the initial BD amount was 5×10^{-4} mol, the sample was named PTFE/BD(5×10^{-4}). The surface density was estimated to be 2.1×10^{-4} g/m^2 for PTFE/BD(5×10^{-4}). The initiation point concentration was 3.2×10^{16} number/m^2. The degrees of polymerization were calculated to be 71 [16]. The tethered PBD chains existed in a dilute situation and were isolated from each other in this work. Although the chain length depended on the initial monomer concentration, the degree of polymerization was approximately 60 ± 10 for PTFE/BD [16]. For the PTFE/IP and PTFE/MPD specimens, it is still difficult to measure the surface density. However, the surface density of PTFE/IP and PTFE/MPD was considered to be very small because of the low concentration of the initial monomer as well as that of the PTFE/BD.

E.s.r. spectra were observed at a low microwave power, in order to avoid power saturation, and with 100 kHz field modulation using JEOL JES-FE3XG and RE1XG spectrometer (X-band) coupled to a temperature controller. The signal of 1,1-diphenyl-2-picrylhydrazyl was used as a *g*-value standard. The magnetic field was calibrated with the well-known splitting constants of Mn^{2+} in MgO.

A spectral simulation program developed by Hori et al. [17] employs the line shape equation derived by Heinzer [18] based on a density matrix theory in the Loiuville representation. Heinzer's equation is identical with that derived from the modified Bloch equation [19]. Sakaguchi et al. have modified the program to simulate e.s.r. spectra of allyl radicals. The radical structure was assumed as shown in Fig. 1. C_α, C_β, C_γ, C_δ, H_α, H_β and H_γ atoms were preliminarily set on the same plane A. C_α–$H_{\alpha1}$, C_α–$H_{\alpha2}$, C_β–H_β and C_γ–H_γ bond axes are put at the position of the C_γ–C_α direction with −90, 30, 90 and −90°, respectively. Fig. 1b shows the two conformations of the ally radicals that have conformation 1 and 2. θ_1 and θ_2 are the dihedral angles of the C_δ–H_δ bond axis relative to the P_π axis that is perpendicular to the plane A.

3. Result and discussion

3.1. Assignments of e.s.r. spectra

Fig. 2 shows the e.s.r. spectra of PTFE/BD(5.1×10^{-4})

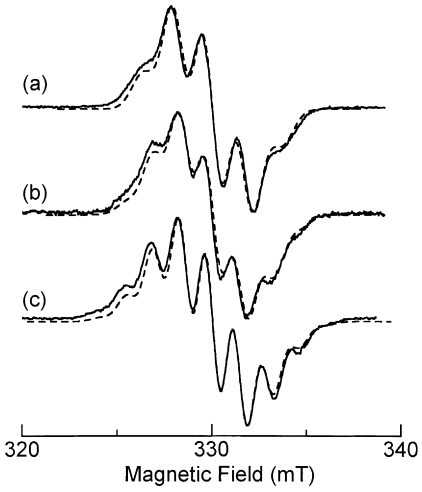

Fig. 2. (a) E.s.r. spectra of end radicals of diene polymers for PTFE/BD (5.1×10^{-4}); (b) PTFE/IP (6.3×10^{-4}); and (c) PTFE/MPD (3.4×10^{-4}). The measurements were carried out at 77 K.

(Fig. 2a), PTFE/IP(6.3×10^{-4}) (Fig. 2b) and PTFE/MPD(3.4×10^{-4}) (Fig. 2c) specimens observed at 77 K which were five-, seven- and nine-line spectra, respectively. The broken lines were simulated spectra assuming a structure as in Fig. 1. E.s.r. parameters were listed in Table 1. The e.s.r. spectral simulation was based on the frozen structures of the free radical given in Fig. 1a and b, which have conformations 1 and 2. The true anisotropic hyper fine splitting (hfs) constants of protons could not be determined because of the broad line width. Thus, the simulation was carried out assuming that the anisotropic hfs's were included in the line width and that the hfs's were isotropic. The spectrum in Fig. 2a had been identified to be end allyl radical of PBD in our previous paper [8].

The spectrum in Fig. 2b was assigned to the PIP end allyl radicals that have a large hfs constant of ca. 1.4 mT and a small hfs of ca. 0.4 mT. In the case that the structure in Fig. 1a is considered, the hfs constant due to β protons (H_β) is small because of the small spin density on the β carbon (C_β).

Table 1
Proton hyperfine splitting constants used in the spectral simulations

Position of protons[a]	PTFE/BD (mT)	PTFE/IP (mT)	PTFE/MPD (mT)
α_1	1.50	1.35	1.42
α_2	1.68	1.35	1.37
β	0.40	0.40	0.40
γ	1.50	1.35	1.37
δ_1[b]	0.50	0.48	0.48
δ_2[b]	1.67	1.61	1.61
$B\rho_c$[b]	3.03	2.92	2.92

[a] α_1, α_2, β, and γ are the protons for BD, γ is the methyl group for IP and α_2 and γ are the methyl groups for MPD.

[b] Hfs's of δ_1 and δ_2 protons are obtained when $\theta_1 = 42°$ and $\theta_2 = 66°$ in the McConnell equation, $A_{H_\delta} = B\rho_c \cos^2\theta$, respectively. Each proton corresponds to one in Fig. 1.

The splitting due to H_β was not well resolved for the broad line width. The hfs constants due to the two H_αs and methyl protons were assumed to be almost equivalent, 1.35 mT. In addition, the hfs constant of H_δ obeys the McConnell equation [20]:

$$A_{H_\delta} = B\rho_c \cos^2\theta$$

where B is an empirical parameter, ρ_c a spin density on C_δ and θ a dihedral angle of the C_δ–H_δ bond axis relative to the P_π axis (see Fig. 1). The hfs constants due to two H_δs were calculated to be 0.48 and 1.68 mT assuming $\theta_1 = 66°$ and $\theta_2 = 42°$, respectively, where the $B\rho_c$ was assumed to be 2.92 mT. One of the A_{H_δ} is so small that the splitting cannot be observed for the broad line width. As a result, six protons—having almost equal hfs constants of 1.4 mT—result in a seven-line spectrum. The calculated spectrum in Fig. 2b using the e.s.r. parameters is in good agreement with the observed results.

The spectrum of nine lines in Fig. 2c was assigned to the PMPD end allyl radicals. The spectrum can be explained by assuming an equivalent hfs constant of 1.4 mT contributed by eight protons. In the case of the structure in Fig. 1a, the free radical has six protons of two methyl groups, one β_1, one γ_2 and two δ protons. The hfs constants because of H_β and one of H_δ are too small to be well resolved for the same manner as the PB and PIB radicals. Therefore, the eight protons with almost equal hfs of 1.4 mT result in a nine-line spectrum. The calculated spectrum agrees with the observed one. All of these e.s.r. parameters used in the simulation are reasonable for allyl type radicals [21,22].

Two possibilities (routes A and B in Fig. 1c) are considered in the attack of radicals to asymmetric IP and MPD monomers. If possibility B occurs, there is no allylic β proton in the B-type radical. The e.s.r. spectra cannot be interpreted by assuming the B-type radical. We can conclude that the propagating radical of PIP and PMPD has an A-type structure in Fig. 1c. These findings show the radical attack mainly on IP and MPD at the 1-position of the monomers. The reason why an A-type structure is predominant over the B-type is probably attributed to the stabilization of the propagating radical by a hyperconjugation with methyl group. For PMPD, the radical attack at 1-position of MPD monomer dominates over 4-position because of both the stabilization of propagating radicals by the hyperconjugation with methyl group and the steric effect of the methyl group bond to its 4-position. These results concerned with the radical attacks of IP and MPD in the solid state polymerization were the same as the results in the liquid state reported by Kamachi et al. [23].

3.2. Molecular mobility of diene polymers tethered on the PTFE surface

Figs. 3–5 show the temperature-dependent e.s.r. spectra for PTFE/BD(5.1×10^{-4}), PTFE/IP(6.3×10^{-4}) and PTFE/MPD(3.4×10^{-4}) specimens, respectively. The spectral

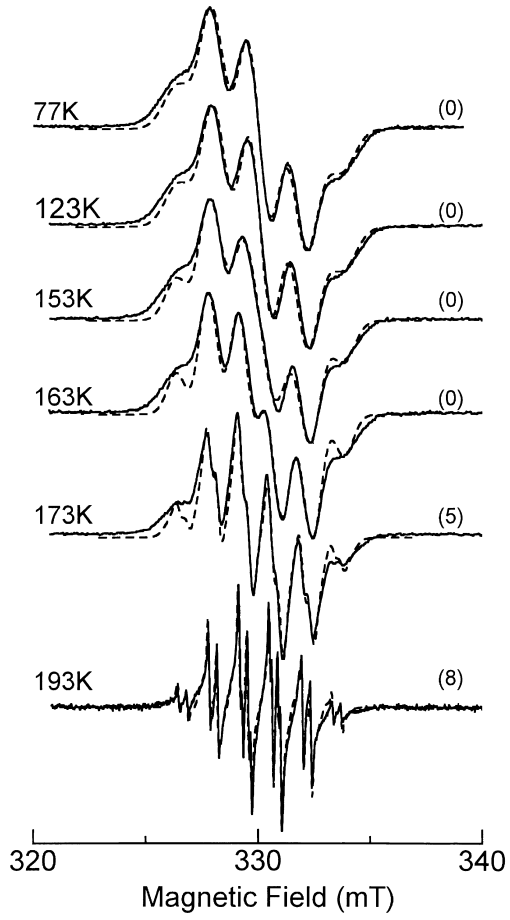

Fig. 3. Temperature-dependent e.s.r. spectra of end radicals for PTFE/BD(5.1×10^{-4}) specimen. The broken lines were simulated by assuming the exchange motion, the motional narrowing and the free rotation. The exchange frequencies were assumed to be null, null, 77, 167, 192 and 250 MHz, in order, from the top spectrum to the bottom one. Values in the brackets indicate the fractional amount (%) of the rotational motion mode.

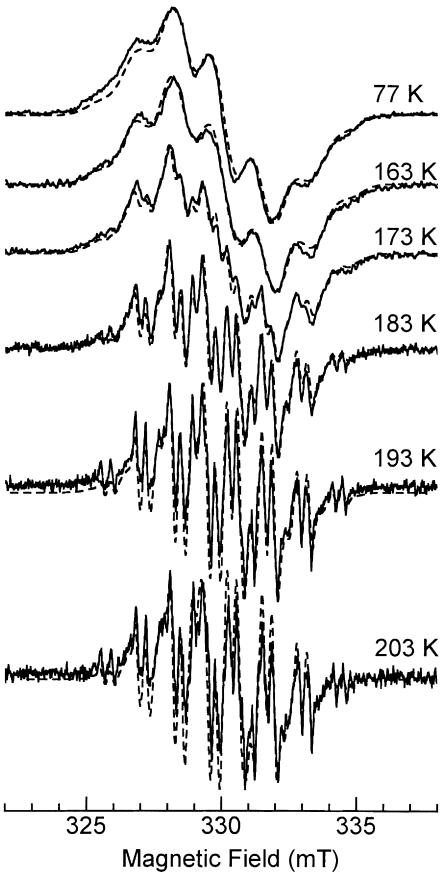

Fig. 4. Temperature-dependent e.s.r. spectra of end radicals for PTFE/IP(6.3×10^{-4}) specimen. The broken lines were simulated by assuming the exchange and the motional narrowing. The exchange frequencies were assumed to be null, 16.7, 33.3, 66.7, 143 and 250 MHz, in order, from the top spectrum to the bottom one.

change from five to six (6×2) lines with temperature was observed for PTFE/BD(5.1×10^{-4}). The spectral change was reversible in the temperature range from 77 to 213 K. The e.s.r. spectral simulation was performed in order to elucidate the change in detail. The broken lines were the simulated spectra using the e.s.r. parameters in Table 1 and assuming some motions. The change at lower temperatures from BD melting point was interpreted in terms of a conformation exchange motion between two sites (vibrational motion) around the C_γ–C_δ bond indicated in Fig. 1b. The frequencies of the conformation exchange are shown in the figure caption. The spectral change in the higher temperature range is attributed to an additional rotational motion around the C_γ–C_δ bond and the rotation of the overall radical itself (motional narrowing). For instance the e.s.r. spectrum at 193 K is very sharp and well resolved because of the rapid molecular motions. The calculated spectrum never fit the observed one at 193 K in Fig. 3 by assuming only the conformation exchange motion. In the conformation exchange mode, the line width and the rate of the exchange motion were varied in order to simulate the spectra. In the rotational motion, however, the calculated spectra using the e.s.r. parameters in Table 1 could not fit the sharp e.s.r. spectra in the higher temperature range. The e.s.r. spectrum at 193 K was simulated using the hfs values of 1.35 for α_1, γ, δ protons, the hfs of 1.47 for α_2 proton, the hfs of 0.37 mT for β proton and a $B\rho_c$ of 2.70 mT. In general, the proton hfs depends on the spin density (ρ_c). In this case, the spin density in the exchange mode may be different from that in the rotational mode, which is considered to be related to a structure (environment) of the PBD chain on the PTFE surface (this is not clear). The simulations were successful since the simulated spectra were in good agreement with the observed ones when the exchange mode of $92 \pm 2\%$ and the rotation mode of $8 \pm 2\%$ were assumed. The allyl radicals of the PBD chains tethered on the PTFE surface have very high mobility even at a low temperature. The radical did not decay at this temperature for at least 20 min. The reason why the radicals were stable in spite of the high mobility is because the PBD chains can be considered to exist in an extremely dilute

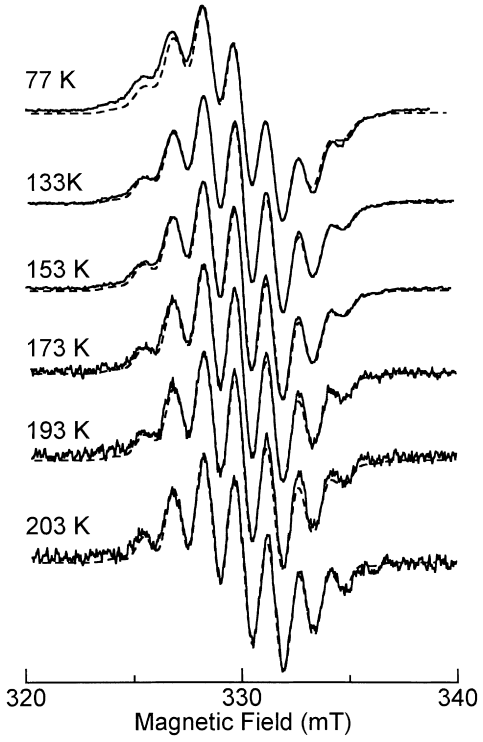

Fig. 5. Temperature-dependent e.s.r. spectra of end radicals for PTFE/MPD(3.4×10^{-4}) specimen. The broken lines were simulated by assuming line width narrowing.

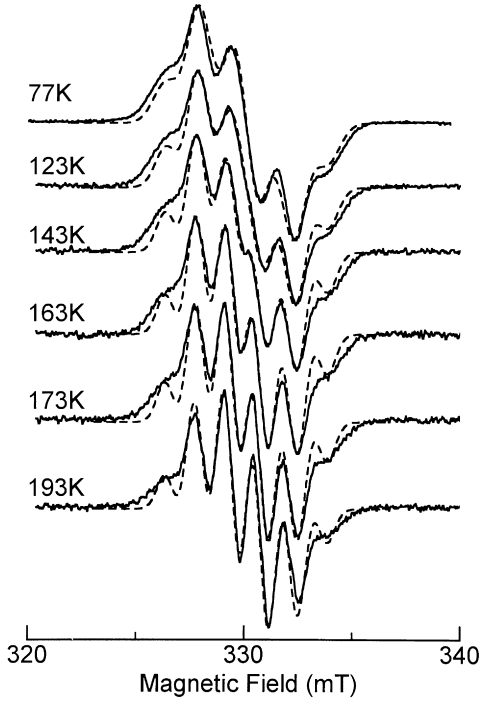

Fig. 6. Temperature-dependent e.s.r. spectra of end radicals for r-PTFE/BD (5.1×10^{-4}) specimen. The broken lines were simulated by assuming the exchange motion and the motional narrowing. The exchange frequencies were assumed to be 38.5, 80, 154, 222, 250 and 417 MHz, in order, from the top spectrum to the bottom one.

situation and because one chain end is tethered onto the PTFE surface.

In the case of PTFE/IP(6.3×10^{-4}) specimen, similarly, a spectral change from seven to eight (nearly 8×2) lines was observed (Fig. 4). The broken lines were the simulated spectra using the e.s.r. parameters in Table 1, assuming the conformation exchange motion and line-width narrowing. The calculated spectrum by assuming the rotational motion mode never fit the observed one for any PTFE/IP specimen. The spectrum at 203 K was not completely 8×2 lines. If the free rotational motion had occurred, the spectrum would clearly be 8×2 lines. Therefore, the rotational motion of the allyl radicals of the PIP on the PTFE surface did not occur.

In contrast with the case of both PTFE/BD and PTFE/IP specimens, the spectral change for PTFE/MPD(3.4×10^{-4}) specimen is little observed except for a slight line-width narrowing. The simulated spectra (broken lines) using the e.s.r. parameters in Table 1 were good agreement with the observed ones (Fig. 5). This finding shows that a rapid rotational motion did not occur in the given temperature range. Only a slow exchange or a very slow rotational motion of the overall allyl PMPD end radicals might occur since these motions were considered to slightly induce the line-width narrowing.

In conclusion, the order of a barrier height of the rotational motion was BD > IP > MPD allyl radicals, which is ascribed to a steric effect of allyl radicals associated with the methyl groups. These rotational motions can be regarded as an intrinsic internal flexibility of the isolated diene polymers on the PTFE surface.

3.3. Influence of segmental density and residual monomer on the molecular motion of end allyl radicals of diene polymer on the PTFE surface

The effect of segmental density on the conformation exchange motion of the PBD chains tethered on the PTFE surface had been reported below the melting point of BD monomer that was present around the PBD chains [8]. The solid monomer was found to restrict the exchange motion. The influence of the residual monomer on the molecular motion of the radicals above the melting point is reported here.

Fig. 6 shows the temperature dependent e.s.r. spectra of PTFE/BD(5.1×10^{-4}) specimens after removing residual monomer that did not polymerize. The sample will be named r-PTFE/BD(5.1×10^{-4}). The elimination made the monomer amount around the PBD chain extremely low, that is, the segmental density was extremely low. It is clear that the spectra in Fig. 6 were not resolved but the rate of the exchange was high below 163 K as compared with the spectra in Fig. 3. Above 163 K, the spectra became sharp for PTFE/BD(5.1×10^{-4}) and the end radicals rotated freely, while the end radicals for r-PTFE/BD(5.1×10^{-4}) did not show the rotational motion. Although the chain length of

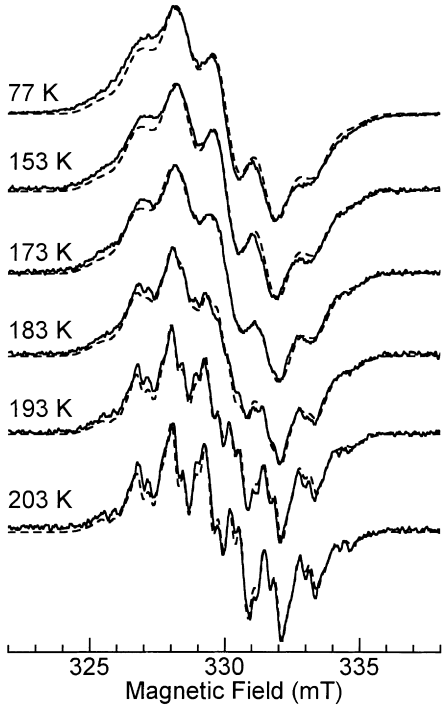

Fig. 7. Temperature-dependent e.s.r. spectra of end radicals for PTFE/IP (5.0×10^{-5}) specimen. The broken lines were simulated by assuming the exchange motion and the motional narrowing. The exchange frequencies were assumed to be null, null, 16.7, 23.8, 50 and 100 MHz, in order, from the top spectrum to the bottom one.

PBD chain on PTFE decreased with a decrease in the initial monomer concentration [16], the temperature-dependent e.s.r. spectra for r-PTFE/BD specimens with a different monomer concentration was identical (not shown). Namely, the chain length had no influence on the mobility of the chain-end in this study. Therefore, these results suggest a plasticizer effect of the monomer on the molecular motion of the PBD on the PTFE, i.e. the enhancement of the molecular mobility. The temperature-dependent e.s.r. spectra for PTFE/IP(5×10^{-5}) specimens are shown in Fig. 7, in which the initial monomer amount was very small. The line width also became broad with a decrease in the initial amount of IP monomer as compared with the spectra in Fig. 4. The site exchange rates of PTFE/IP (6.3×10^{-4}) were higher than that of the PTFE/IP(5×10^{-5}) specimen above 173 K. The enhancement of the exchange motion of the PIP was observed for PTFE/IP (6.3×10^{-4}) specimens as shown in Fig. 4. The monomer concentration dependence of the spectra below 163 K was not observed in spite of being above the melting point of the IP monomer (near 133 K). Therefore, the effect of the residual monomer is detected very less in the solid or viscous states below 163 K, which is different from the case of the PTFE/BD specimens. The change of the spectral pattern and the line sharpness was almost the same for both PTFE/BD and PTFE/IP specimens when the initial monomer was more than 5.0×10^{-4} mol. That is, the further enhancement of the mobilities was not observed. On the other hand, for PTFE/MPD specimens, the monomer concentration dependence of the e.s.r. spectra was almost not observed in the given temperature range. This is because the mobility of the PMPD end radical is relatively low.

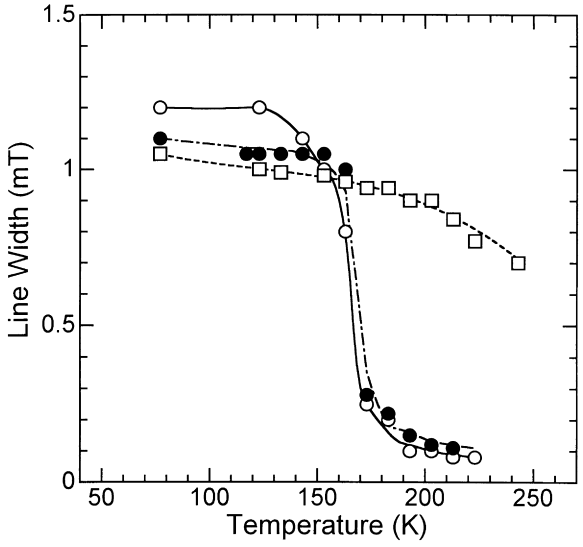

Fig. 8. Temperature dependence of the line width for PTFE/BD (5.1×10^{-4}) (open circle), PTFE/IP (6.3×10^{-4}) (solid circle) and PTFE/MPD (5.5×10^{-4}) (square) specimen.

Fig. 8 shows the temperature dependence of the line width obtained by simulation for PTFE/BD (5.1×10^{-4}) (open circles), PTFE/IP (6.3×10^{-4}) (solid circles) and PTFE/MPD(5.5×10^{-4}) (squares) specimens. For PTFE/BD and PTFE/IP specimens, the line widths narrow drastically in the temperature range of 150 to 170 K, while no drastic change of the line width for the PTFE/MPD specimen was observed. The line-width narrowing is considered to be associated with the 3D random motion of the overall radical. The narrowing of the line width, which is not shown in Fig. 8 but clear in Fig. 6, for the monomer-removed sample (r-PTFE/BD) was almost not observed. This narrowing indicates the plasticizer effect of the molecular motion by the monomer. Although the viscosity of each monomer was not definite, we suggest that the order of the mobility can be determined for each radical.

Usually, in the temperature region where motional narrowing of the line width of the magnetic resonance (e.s.r., n.m.r.) spectrum occurs, the correlation time associated with the corresponding molecular motion can be obtained by the BPP equation [24], the related activation energies can also be calculated. According to the modified BPP equation by Gutowsky and Meyer [25], the relationship between the frequency of the motion and line width can be given as follows.

$$(\Delta\nu)^2 = M^2 + (R^2 - M^2)\frac{2}{\pi}\tan^{-1}\left(\frac{\alpha\Delta\nu}{\nu_c}\right)$$

where M is the line width in 3D random motion state, R is the line width in rigid state and ν_c is a correlation frequency giving the average rate of change in structural configuration. α is a

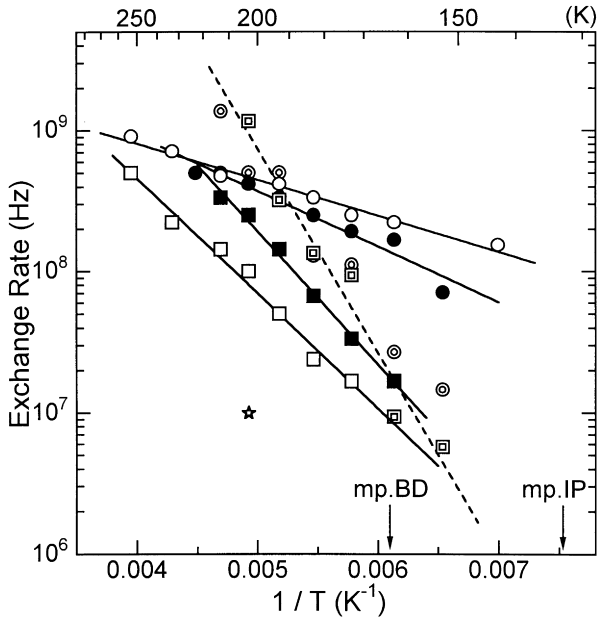

Fig. 9. Arrhenius plots of the exchange rate for r-PTFE/BD (5.1×10^{-4}) (open circle), PTFE/BD (5.1×10^{-4}) (solid circle), PTFE/IP (6.3×10^{-4}) (solid square) and PTFE/IP (5.0×10^{-5}) (open square) specimens. The motional narrowing (3D motion) are shown for PTFE/BD (5.1×10^{-4}) (dual circles) and PTFE/IP (6.3×10^{-4}) (dual squares). Star marks show the rate when the site exchange could be assumed for PTFE/MPD (5.5×10^{-4}) specimen. The melting points of BD and IP are marked with arrows.

line width parameter (assumed to be unity) and $\Delta\nu$ is the observed line width at the transition (narrowing) temperature region. The line widths are all given in a frequency scale. Using this equation, the correlation frequencies of the free radicals were calculated and shown in Fig. 9 for PTFE/BD (dual circles) and PTFE/IP (dual squares). The activation energy was calculated to be ca. 6.6 kcal/mol.

The average rates of the conformation exchange motion for PTFE/BD (5.1×10^{-4}) (solid circles) r-PTFE/BD (5.1×10^{-4}) (open circles), PTFE/IP (6.3×10^{-4}) (solid squares) and PTFE/IP(5.0×10^{-5}) (open squares) were also plotted in Fig. 9. The apparent activation energies were estimated to be 1.9, 1.2, 4.3 and 3.7 kcal/mol for PTFE/BD (5.1×10^{-4}), r-PTFE/BD (5.1×10^{-4}), PTFE/IP (6.3×10^{-4}) and PTFE/IP (5.0×10^{-5}) specimens, respectively.

The frequency (ν_{ex}) of the conformation exchange motion was about six times higher than that of the motional narrowing (ν_c) (3D random motion) at 163 K for PTFE/BD (5.1×10^{-4}). In contrast, at 213 K, the ν_c was 2.7 times as high as ν_{ex}. For PTFE/IP (6.3×10^{-4}), ν_c was much higher than ν_{ex} in the almost any given temperature range. The 3D motion is responsible for the coupling of accumulation of a vibration (exchange) around every C–C bond and a displacement of the whole radical in a larger scale. The exchange motion is a local motion and is associated with the internal flexibility of the polymer chain. The displacement in a larger scale is induced by the residual liquid monomer in this case, which is probably related to the intermolecular interaction between the monomer and the polymer chain. The PBD chains are consequently supposed to be more flexible than the PIP chains.

In addition, for PTFE/BD system, below the melting point of the BD monomer, the solid monomer restricted the exchange motion of the BD allyl radicals and the activation energy was higher in the presence of the solid monomer than in the absence of the residual monomer. In the presence of the residual monomer, the free rotation around C_γ–C_δ occurred and the line width decreased steeply above the melting point of BD. The e.s.r. spectra observed due to the freely rotating motion was remarkable in the spectra in this temperature region. The exchange rates were smaller for the PTFE/BD (5.1×10^{-4}) than for the r-PTFE/BD (5.1×10^{-4}) in the higher temperature region as shown in Fig. 9. It was considerably hard to determine the precise rates of exchange since the sharp e.s.r. spectra observed due to the rotation motion for the PTFE/BD (5.1×10^{-4}) in this region was remarkable. Hence, in this region, it is not very important to discuss the difference of the exchange rates for each sample. For the PTFE/IP system, the conformation exchange motion was enhanced by the plasticizer effect of the residual monomer. Especially above 173 K (far above melting point) the 3D motion was enhanced. The freely rotating motion, which is associated with a high-energy barrier of the rotation, was not observed in the given temperature range. In the temperature range of 133–163 K in spite of being above the melting point of IP, the well-resolved spectra that may be associated with a viscous liquid of IP were not observed in the temperature range. The star mark indicates the ν_{ex} of the MPD free radical when the exchange motion could be assumed to induce the spectral change (slight line-width narrowing). The comparison of the ν_{ex} at 203 K for each free radical clearly shows that the ν_{ex} of the MPD radical is lower than that of the others by a factor of ten.

4. Conclusion

The molecular mobilities of end allyl radicals of diene polymers tethered on a PTFE surface were studied by the e.s.r. method. The following findings were obtained.

1. For the PTFE/BD, three types of motions of end allyl radicals of the PBD were observed: (a) the conformation exchange motion around the C_γ–C_δ bond, (b) the free rotation around the C_γ–C_δ bond and (c) the 3D random motion. The solid residual monomers restricted the exchange motion and the liquid monomers enhanced the motions.
2. For the PTFE/IP, two types of motions of end allyl radicals of the PIP were observed: (a) the conformation exchange and (b) the 3D random motion. The effect of the residual monomer (the enhancement of the exchange motions) was observed above 163 K. However, no free rotational motion was observed.
3. For PTFE/MPD, the line width decreases slightly with

temperature and the mobility of the end allyl radicals was the lowest. The residual monomers did not influence the mobility.

From these findings, it was found that the order of the mobility at the end allyl radicals of the diene polymers on the PTFE surface was PB > PIP > PMPD. The rotational barrier around C_γ–C_δ for PBD end radicals is the lowest, owing to an absence of a methyl groups in the monomer unit and that for PMPD is the highest, owing to the presence of two methyl groups in the monomer unit. The internal flexibility of the isolated single chains of the diene polymers did not follow the order of their glass transition temperatures. It was concluded that bulk properties were determined by the addition of some intermolecular interactions to the intramolecular interaction.

Acknowledgements

This work was supported by a Research Fellowship of the Japan Society for the Promotion of Science for Young Scientists.

References

[1] Kumaki J, Nishikawa T, Hashimoto T. J Am Chem Soc 1996;118:3321.
[2] Pilcher SC, Ford WT. Macromolecules 1998;31:3454.
[3] Qian R, Shen J, Bei N, Bai C, Zhu C, Wang X. Macromol Chem Phys 1996;197:2165.
[4] Zhang LS, Manke CW, Ng KYS. Macromolecules 1995;28:7386.
[5] Chen L, Ni N, Jia S, Jin X, Ge S, Takahara A, Kajiyama T. J Macromol Sci Phys 1998;B37(3):339.
[6] Ortiz C, Hadziioannou G. Macromolecules 1999;32:780.
[7] Yamamoto K, Shimada S, Ohira K, Sakaguchi M, Tsujita Y. Macromolecules 1997;30:6575.
[8] Yamamoto K, Shimada S, Tsujita Y, Sakaguchi M. Polymer 1997;38:6327.
[9] Sakaguchi M, Shimada S, Yamamoto K, Sakai M. Macromolecules 1997;30:8521.
[10] Sakaguchi M, Shimada S, Yamamoto K. J Polym Sci, Part B Polym Phys 1998;36:2095.
[11] Sakaguchi M, Shimada S, Yamamoto K. Macromolecules 1998;31:7829.
[12] Sakaguchi M, Sohma J. J Appl Polym Sci 1978;22:2915.
[13] Sakaguchi M, Shimada S, Yamamoto K. Macromolecules 1997;30:3620.
[14] Kurokawa N, Sakaguchi M, Sohma J. Polym J 1978;10:93.
[15] Sakaguchi M, Sohma J. J Polym Sci Polym Phys Ed 1975;28:973.
[16] Yamamoto K, Shimada S, Sakaguchi M, Tsujita Y. Polym J 1997;29:370.
[17] Hori Y, Shimada S, Kashiwabara H. J Phys Chem 1986;90:3037.
[18] Heinzer. J Mol Phys 1971;22:167.
[19] Bloch F. Phys Rev 1946;70:460.
[20] Heller C, McConnell HM. J Chem Phys 1960;32:1535.
[21] Ohmori T, Ichikawa T, Iwasaki M. Bull Chem Soc Jpn 1973;46:1383.
[22] Fessenden RW, Schuler RH. J Chem Phys 1963;39:2147.
[23] Kamachi M, Kajiwara A. Macromolecules 1996;29:2387.
[24] Bloembergen N, Purcell EM, Pound RV. Phys Rev 1948;73:679.
[25] Gutowsky HS, Meyer LH. Chem Phys 1953;21:2122.